Available online at www.sciencedirect.com
SCIENCE DIRECT®
Journal of Nuclear Materials 323 (2003) 380–387
journal of nuclear materials
www.elsevier.com/locate/jnucmat

Influence of stress fields of dislocations on formation and spatial stability of point defects (elastic dipoles) in V and Fe crystals

A.B. Sivak [a], V.A. Romanov [b], V.M. Chernov [a,*]

[a] SSC-RF, A.A. Bochvar Institute of Inorganic Materials, Moscow 123060, P.O. Box 369, Russia
[b] A.I. Leypunskiy Institute of Physics and Power Engineering, Obninsk, Russia

Abstract

Formation energies, dipole forces and crystallographic characteristics of point defects (vacancies and self-interstitial atoms) as elastic dipoles of different symmetry were defined for bcc V and Fe crystals by computer simulation methods with use of modified interatomic interaction potentials. Stress fields and energy factors of screw, mixed (45°) and edge dislocations in basic slip system of V and Fe crystals $\langle 1\,1\,1\rangle\{1\,1\,0\}$ were calculated in the framework of the anisotropic theory of elasticity. Elastic interaction energies of the above mentioned point defects and dislocations were calculated and the essential influence of these interactions (for vacancies via their saddle point positions especially) on formation energies, crystallographic configurations (stable and unstable) and diffusion ways of point defects was shown. Critical densities of dislocations were defined, at which their stress fields control the thermal mobility of point defects throughout the whole crystal volume.

PACS: 61.71.Ji; 61.72.Lk; 61.80.Az

1. Introduction

The development of physical models of all functional properties (strength, plasticity, embrittlement, swelling, etc.) of structural materials under irradiation demands a detailed knowledge of the properties of point defects, dislocations and their interactions in such materials (real anisotropic crystals with different crystallographic symmetries). In spite of its importance, the problem of formation, interactions and mobility of point defects and dislocations is not investigated well enough to quantitatively predict the evolution of point defects and dislocations under irradiation (bias factors, etc.) in real anisotropic crystals with different types of point defects (elastic dipoles) and dislocations [1–4].

In this work, the formation energetics of self point defects (vacancies, self-interstitial atoms (SIAs) as elastic dipoles of different symmetries) with respect to crystallography and interactions with screw, mixed 45° and edge dislocations (SD, MD and ED respectively) in $\langle 1\,1\,1\rangle\{1\,1\,0\}$ basic slip system was studied for bcc crystals V and Fe, which are the basis element of advanced structural materials (low activated, in that number) for fusion and fission power reactors. Besides, Fe and V crystals are typical bcc crystals with different factors of elastic anisotropy $A = 2c_{44}/(c_{11} - c_{12})$ which are 2.36 and 0.78 for Fe and V (room temperature), respectively (c_{11}, c_{12}, c_{44} are elastic constants). Therefore, the study of defects in these crystals allows to estimate the role of elastic anisotropy in the formation of defect microstructure of bcc crystals.

Computer simulation methods (for calculation of point defects characteristics in crystals without dislocations) and the linear anisotropic theory of elasticity (for calculations of elastic fields of dislocations and their

* Corresponding author. Tel.: +7-095 190 3605; fax: +7-095 196 4168.
E-mail address: chernovv@bochvar.ru (V.M. Chernov).

0022-3115/$ - see front matter © 2003 Elsevier B.V. All rights reserved.
doi:10.1016/j.jnucmat.2003.08.014

interactions with point defects) were used both for calculations of interaction of point defects with dislocations [3,5–9].

2. Elastic stress fields of dislocations

Dislocation stress fields σ_{ij} (i, $j = 1$, 2, 3, define the coordinate axes in a dislocation coordinate system where the axis 3 is along a dislocation) and energy factors $K(\varphi)$ (φ is an angle between the direction of the dislocation and Burgers vector **b**) of arbitrary oriented straight dislocations (SDs, MDs, EDs) in basic slip systems of bcc crystals $\{1\,1\,0\}\langle 1\,1\,1\rangle$, $\{1\,1\,2\}\langle 1\,1\,1\rangle$) were calculated for V and Fe crystals in the framework of anisotropic theory of elasticity following algebraic method [1,7]. Values of Fe and V elastic constants (sometimes with extrapolation) were taken from [1,10,11]. There is a feature in bcc crystals ($\langle 1\,1\,1\rangle$ Burgers vector) that is absent in fcc crystals ($\langle 1\,1\,0\rangle$ Burgers vector). It is the existence of stress tensor diagonal components of SDs with Burgers vector $\langle 1\,1\,1\rangle$ (dislocation is directed along a symmetry axis of an odd order [1,6]). Calculated polar diagrams $K^{-1}(\varphi)$ for above mentioned two basic slip systems in V and Fe crystals at temperature up to 1000 K show the absence of concave regions, i.e. dislocations keep straight forms [1,6].

3. Crystal model and interatomic potentials

The model [12,13] used for studying defects in V and Fe crystals describes the interatomic interactions in the framework of pair central-symmetric interaction potentials and takes into account effects of electron density redistribution (effective accounting of non-central and many-body interactions) by introducing a volume dependent additive component into the crystal energy density. The behaviour and properties of point defects disturbing the crystal lattice and the results of modelling of their properties essentially depend on the form (especially on the repulsive part) of the potential. Therefore the procedure of parameterization of the V–V and Fe–Fe potentials included not only the condition of exact accordance to equilibrium crystal properties (experimental values of lattice constant and elastic constants) but the condition of satisfaction to the equation of state of crystals under high pressures [14–16] and the condition of asymptotic transition of analytical form of the calculated potential to the universal Coulomb interaction screening potential [17]. Fig. 1 is a plot of interatomic potentials in V and Fe crystals calculated in the framework of the above-stated algorithm.

The computational cell is a cube of size 11 lattice parameters on edge under a fixed boundary condition. Such sizes of the computational cell ensured accuracy of calculations of characteristics of point defects within the limits of 0.5%.

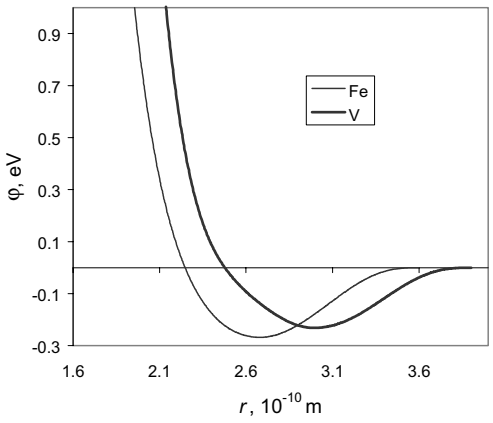

Fig. 1. Interatomic potentials in bcc Fe and V crystals.

A point defect in a crystal lattice causes surrounding atoms to be displaced from their ideal positions, thus determining the configuration of the elastic dipole produced in the lattice and characterized by dipole tensor P_{ij} [2,3,5]. The tensor P_{ij} is represented in terms of the three eigenvalues $P^{(s)}$ ($s = 1$, 2, 3) and eigenvectors $\mathbf{e}^{(s)}$ since the principal axes $\mathbf{e}^{(s)}$ are completely determined by the local symmetry of the defect configuration. The symmetry of the resulting defect configuration (tetragonal $\langle 1\,0\,0\rangle$, trigonal $\langle 1\,1\,1\rangle$, orthorhombic $\langle 1\,1\,0\rangle$ in dependence on the eigenvalues $P^{(1)}$, $P^{(2)}$, $P^{(3)}$), as a rule, is lower than the local symmetry of the bcc lattice. This implies the presence of N crystallographically equivalent orientations of the elastic dipoles (orientations A, B,...,F, Table 1). The number N of such orientations corresponds to the specified principal eigenvector $\mathbf{e}^{(1)}$ [3,9].

Calculations of dipole tensors and relaxation volumes of point defects were performed using algorithms [18,19]. Tables 2 and 3 list calculated values of the formation energies E^{F}, the relaxation volumes V^{R} and the three eigenvalues $P^{(s)}$ of different point defects as elastic dipoles in Fe and V crystals without internal stresses (without dislocations). The formation energy of a particular point defect configuration in Fe and V crystals increases in different sequences. In Fe crystal: $\langle 1\,1\,0\rangle$ dumbbell, $\langle 1\,1\,1\rangle$ dumbbell, crowdion, tetrahedral,

Table 1
Correspondence of A–F elastic dipoles configurations to the crystallographic directions in a bcc crystal for different values N

N	A	B	C	D	E	F
6	[1 1 0]	[$\bar{1}$ 1 0]	[0 1 1]	[0 1 $\bar{1}$]	[1 0 1]	[$\bar{1}$ 0 1]
4	[1 1 1]	[$\bar{1}$ 1 1]	[1 $\bar{1}$ 1]	[1 1 $\bar{1}$]		
3	[1 0 0]	[0 1 0]	[0 0 1]			

Table 2
Characteristics of the point defect configurations (elastic dipoles) in Fe

Configuration	E^F, eV	V^R, Ω	$P^{(1)}$, eV	$P^{(2)}$, eV	$P^{(3)}$, eV	$\mathbf{e}^{(1)}$	$\mathbf{e}^{(2)}$	$\mathbf{e}^{(3)}$	N
⟨1 1 0⟩ dumbbell	5.20	1.47	22.94	12.98	20.33	(1 1 0)	(−1 1 0)	(0 0 1)	6
⟨1 1 0⟩ dumbbell saddle point	5.45	1.47	27.73	15.59	12.78	(1 1.11 1)	(1 0 −1)	(1 −1.8 1)	
⟨1 1 1⟩ dumbbell	5.42	1.43	30.91	11.80	11.80	(1 1 1)	(1 −1 0)	(1 1 −2)	4
⟨1 0 0⟩ dumbbell	6.26	1.16	19.77	12.28	12.28	(1 0 0)	(0 1 0)	(0 0 1)	3
Octahedral	6.11	1.17	21.01	11.77	11.77	(1 0 0)	(0 1 0)	(0 0 1)	3
Tetrahedral	5.86	1.28	15.52	16.65	16.65	(1 0 0)	(0 1 0)	(0 0 1)	3
Crowdion	5.44	1.43	30.89	11.92	11.92	(1 1 1)	(1 −1 0)	(1 1 −2)	4
Vacancy	1.85	−0.13	−1.69	−1.69	−1.69	(1 0 0)	(0 1 0)	(0 0 1)	1
Vacancy saddle point	2.59	−0.08	−3.33	0.11	0.11	(1 1 1)	(1 −1 0)	(1 1 −2)	4
Divacancy$^{\langle 100\rangle}$	3.40	−0.35	−6.05	−3.63	−3.63	(1 0 0)	(0 1 0)	(0 0 1)	3
Divacancy$^{\langle 111\rangle}$	3.63	−0.22	−1.27	−3.64	−3.64	(1 1 1)	(1 −1 0)	(1 1 −2)	4
Di-SIA[a]	9.47	2.83	43.93	23.84	40.08	(1 1 0)	(−1 1 0)	(0 0 1)	6
Di-SIA									
Crowdion (−0.5 −0.5 1.5) + Crowdion (0.5 0.5 0.5)	9.62	2.88	62.07	24.86	22.91	(1 1 0.89)	(−1 1 0)	(1 1 −2.25)	

[a] A couple of ⟨1 1 0⟩ dumbbell configurations which axes are parallel to each other and centres are in the nearest neighbours positions in bcc lattice located along the perpendicular to the dumbbells axes.

Table 3
Characteristics of the point defect configurations (elastic dipoles) in V

Configuration	E^F, eV	V^R, Ω	$P^{(1)}$, eV	$P^{(2)}$, eV	$P^{(3)}$, eV	$\mathbf{e}^{(1)}$	$\mathbf{e}^{(2)}$	$\mathbf{e}^{(3)}$	N
⟨1 1 0⟩ dumbbell	5.76	1.32	21.14	13.36	20.31	(1 1 0)	(−1 1 0)	(0 0 1)	6
⟨1 1 1⟩ dumbbell	5.68	1.07	23.73	10.23	10.23	(1 1 1)	(1 −1 0)	(1 1 −2)	4
⟨1 0 0⟩ dumbbell	4.67	0.67	11.90	7.89	7.89	(1 0 0)	(0 1 0)	(0 0 1)	3
Octahedral	4.93	0.80	14.70	9.13	9.13	(1 0 0)	(0 1 0)	(0 0 1)	3
Tetrahedral	5.36	0.95	13.29	12.95	12.95	(1 0 0)	(0 1 0)	(0 0 1)	3
Crowdion	5.72	1.08	24.02	10.29	10.29	(1 1 1)	(1 −1 0)	(1 1 −2)	4
Vacancy V^I	2.24	−0.28	−3.81	−3.81	−3.81	(1 0 0)	(0 1 0)	(0 0 1)	1
Vacancy V^{IIa}	1.73	−0.62	−8.61	−8.61	−8.61	(1 0 0)	(0 1 0)	(0 0 1)	1
Vacancy saddle point	2.71	−0.26	−5.88	−2.37	−2.37	(1 1 1)	(1 −1 0)	(1 1 −2)	4
Divacancy$^{\langle 100\rangle}$	3.94	−0.65	−9.75	−8.64	−8.64	(1 0 0)	(0 1 0)	(0 0 1)	3
Divacancy$^{\langle 111\rangle}$	4.35	−0.60	−6.54	−9.22	−9.22	(1 1 1)	(1 −1 0)	(1 1 −2)	4
Di-SIA									
Oct(0 0 1) + Oct(1 −1 0)	9.17	1.52	19.44	16.48	27.12	(1 1 0)	(−1 1 0)	(0 0 1)	6
Di-SIA									
Oct(1 0 0) + Oct(0 1 0)	9.41	1.73	25.83	24.93	20.93	(1 1 0)	(−1 1 0)	(0 0 1)	6

[a] This vacancy configuration V^{II} (non-considering further) has lower symmetry order in comparison with vacancy configuration V^I but still keeps spherical symmetry of long-range elastic field.

octahedral, ⟨1 0 0⟩ dumbbell; in V crystal: ⟨1 0 0⟩ dumbbell, octahedral, tetrahedral, ⟨1 1 1⟩ dumbbell, crowdion, ⟨1 1 0⟩ dumbbell. Thus, ⟨1 1 0⟩ and ⟨1 0 0⟩ dumbbells are the most stable point defect configurations in Fe and V crystals without internal stresses (without dislocations) respectively.

4. Interaction of dislocations with point defects (elastic dipoles)

The amplitude and angular functions of the elastic interaction between dislocations and elastic dipoles depend on the types of dislocations. In this study SD, MD and ED with Burgers vector $\mathbf{b} = a/2\ [1\,1\,1]$ (a is the lattice constant) in basic slip system $(\bar{1}\,1\,0)[1\,1\,1]$ were considered.

The formation energy of a point defect configuration in the neighbourhood of a dislocation can change because of the interaction between the point defect and the elastic dislocation field:

$$E_{\mathrm{d}}^{\mathrm{F}} = E^{\mathrm{F}} + E_{\mathrm{int}}(\mathbf{r}), \tag{1}$$

where $E_{\mathrm{d}}^{\mathrm{F}}$ is the formation energy of the point defect in the presence of the dislocation stress field and $\mathbf{r}$ is the radius-vector of the position of the point defect with respect to the dislocation line.

The interaction energy E_{int} within the framework of the theory of elasticity is given by [3,5–9]

$$E_{\mathrm{int}}(\mathbf{r}) = -P_{ij}\varepsilon_{ij}^{\mathrm{d}}(\mathbf{r}) = E_0\frac{b}{r}f(\varphi), \quad \int_0^{2\pi}[f(\varphi)]^2\,\mathrm{d}\varphi = \pi. \tag{2}$$

Here $\varepsilon_{ij}^{\mathrm{d}}$ is the elastic-strain tensor caused by a dislocation, E_0 is the dislocation–point defect binding energy and function $f(\varphi)$ specifies the angular dependence of the interaction energy. Tables 4 and 5 list values of the binding energies E_0 of different point defects configurations.

Taking relations (1) and (2) into account, one can determine the sequence of point defects (elastic dipoles) configurations in ascending sort of their formation energy $E_{\mathrm{d}}^{\mathrm{F}}$ in the presence of different types of dislocations (SD, MD, ED) for different regions specified by the radius-vector $\mathbf{r}$. The configuration that occurs in the neighbourhood of a dislocation should have the lowest energy $E_{\mathrm{d}}^{\mathrm{F}}$. Tables 6 and 7 give the SIA configurations in particular orientations (disorientation angles between Burgers vector and the SIA eigenvector $\mathbf{e}^{(1)}$ are also given) with the lowest formation energy $E_{\mathrm{d}}^{\mathrm{F}}$ in the field of considered dislocations at different distances from the dislocation in Fe and V crystals. Dependencies of formation energy $E_{\mathrm{d}}^{\mathrm{F}}$ of these and some other configurations on distance to the dislocation are shown at Figs. 2–5. Fig. 2 also illustrates that the dislocation stress field inserts a distinction between different orientations of the same point defect configurations.

Table 4
Binding energy E_0 of considered SD, MD and ED in $(\bar{1}\,1\,0)[1\,1\,1]$ slip plane with SIA and vacancy configurations in Fe, eV

Configuration	Orientation	Dislocation type		
		SD	MD	ED
⟨1 1 0⟩ dumbbell	A	0.291	1.621	2.102
	B	0.570	0.808	1.518
	C	0.291	1.631	2.083
	D	0.570	1.170	1.485
	E	0.291	1.631	2.083
	F	0.570	1.170	1.485
⟨1 0 0⟩ dumbbell	A	0.696	1.307	1.502
	B	0.696	1.307	1.502
	C	0.696	0.724	1.452
⟨1 1 1⟩ dumbbell	A	0.191	2.485	3.056
	B	0.747	1.152	1.563
	C	0.747	1.152	1.563
	D	0.747	1.177	1.210
Octahedral	A	0.841	1.410	1.577
	B	0.841	1.410	1.577
	C	0.841	0.662	1.477
Tetrahedral	A	0.282	1.099	1.526
	B	0.282	1.099	1.526
	C	0.282	1.161	1.507
Crowdion	A	0.193	2.481	3.052
	B	0.743	1.153	1.568
	C	0.743	1.153	1.568
	D	0.743	1.182	1.220
Vacancy		0.027	0.116	0.158
Vacancy saddle point	A	0.002	0.294	0.354
	B	0.123	0.163	0.154
	C	0.123	0.163	0.154
	D	0.123	0.098	0.029

4.1. Iron crystal

The radius-vectors delineating regions of stabilization of crowdion and ⟨1 1 1⟩ dumbbell configurations by dislocation elastic fields take on values $r_{\mathrm{s}} \approx 1$ b and $r_{\mathrm{e}} \approx 4$ b for SD and ED, respectively (Table 6).

The migration of a SIA to a SD occurs in the following sequence. As a result of diffusion through the lattice, the SIA far from the SD appears in the neighbourhood of the dislocation, where its ⟨1 1 0⟩ dumbbell configuration is energetically disadvantageous. Therefore, this configuration changes into ⟨1 1 1⟩ dumbbell and crowdion configurations making it easier for the SIA to reach the SD.

Table 5
Binding energy E_0 of considered SD, MD and ED in $(\bar{1}\,1\,0)[1\,1\,1]$ slip plane with SIA and vacancy configurations in V, eV

Configuration	Orientation	Dislocation type		
		SD	MD	ED
⟨1 1 0⟩ dumbbell	A	0.120	1.283	1.763
	B	0.543	0.553	1.012
	C	0.120	1.214	1.550
	D	0.543	0.851	1.167
	E	0.120	1.214	1.550
	F	0.543	0.851	1.167
⟨100⟩ dumbbell	A	0.289	0.588	0.696
	B	0.289	0.588	0.696
	C	0.289	0.328	0.689
⟨1 1 1⟩ dumbbell	A	0.038	1.784	2.241
	B	0.740	0.808	1.035
	C	0.740	0.808	1.035
	D	0.740	0.854	0.904
Octahedral	A	0.401	0.735	0.848
	B	0.401	0.735	0.848
	C	0.401	0.364	0.828
Tetrahedral	A	0.054	0.661	0.929
	B	0.054	0.661	0.929
	C	0.054	0.643	0.932
Crowdion	A	0.038	1.809	2.272
	B	0.753	0.820	1.048
	C	0.753	0.820	1.048
	D	0.753	0.864	0.911
Vacancy		0.014	0.191	0.271
Vacancy saddle point	A	0.009	0.450	0.564
	B	0.192	0.206	0.257
	C	0.192	0.206	0.257
	D	0.192	0.211	0.215

The migration of a SIA to an ED differs from the migration to a SD. The SIA that is far from the dislocation migrates in the direction where its interaction energy with the ED decreases, reaches the neighbourhood $r_e \approx 4$ b where its ⟨1 1 0⟩ dumbbell configuration is energetically disadvantageous. Consequently the SIA forms ⟨1 1 1⟩ dumbbell configuration in the *A* orientation (parallel to the Burgers vector, Table 1), which gives rise to one-dimensional diffusion in the neighbourhood of the ED. The SIA migrates along the [1 1 1] axis in a plane parallel to the slip plane of the ED. The transition of the SIA to a plane, which is closer to the slip plane and, therefore, to the dislocation, requires a considerable energy.

Thus, the qualitative difference between migration of a SIA to an ED or a SD is that the SIA 'hovers' at distances $r_e \approx 4$ b in the neighbourhood of the ED in the form of ⟨1 1 1⟩ dumbbell configuration with the principal axis parallel to the direction of the Burgers vector.

The migration of a vacancy to a dislocation is governed by interaction between the vacancy saddle point configuration (⟨1 1 1⟩ elastic dipole) and the dislocation. The interaction energies demonstrate that vacancy reaches the SD and 'hovers' at some distance from the ED.

4.2. Vanadium crystal

The radius-vectors delineating regions of stabilization of crowdion and ⟨1 1 1⟩ dumbbell configurations by dislocation elastic fields take on values $r_s \approx 0.5$ b and $r_e \approx 1.5$ b for a SD and an ED, respectively (Table 7).

The migration of SIAs and vacancies in V crystal does not qualitative differ from the migration in Fe crystal with the exception of the most stable SIA configuration far from dislocation (⟨1 0 0⟩ and ⟨1 1 0⟩ dumbbell configurations in V and Fe crystals, respectively).

Table 6
SIA configurations with the lowest formation energy E_d^F in the field of SD, MD and ED in $(\bar{1}\,1\,0)[1\,1\,1]$ slip plane at different distances from the dislocation in Fe

r, b	Configuration	Orientation	Disorientation angle ($\mathbf{b}\hat{}\mathbf{e}^{(1)}$)
Screw dislocation			
<0.8	⟨1 1 1⟩ dumbbell or crowdion	B, C, D	70.53°
>0.8	⟨1 1 0⟩ dumbbell	B, D, F	90°
Edge dislocation			
<4.3	⟨1 1 1⟩ dumbbell or crowdion	A	0°
>4.3	⟨1 1 0⟩ dumbbell	A, C, E	35.26°
Mixed 45° dislocation			
<3.9	⟨1 1 1⟩ dumbbell or crowdion	A	0°
>3.9	⟨1 1 0⟩ dumbbell	A, C, E	35.26°

Table 7
SIA configurations with the lowest formation energy E_d^F in the field of SD, MD and ED in $(\bar{1}\,1\,0)[1\,1\,1]$ slip plane at different distances from the dislocation in V

r, b	Configuration	Orientation	Disorientation angle ($\mathbf{b}\hat{}\mathbf{e}^{(1)}$)
Screw dislocation			
<0.5	⟨1 1 1⟩ dumbbell or crowdion	B, C, D	70.53°
>0.5	⟨1 0 0⟩ dumbbell	A–C	54.74°
Edge dislocation			
<1.6	⟨1 1 1⟩ dumbbell or crowdion	A	0°
>1.6	⟨1 0 0⟩ dumbbell	A–C	54.74°
Mixed 45° dislocation			
<1.2	⟨1 1 1⟩ dumbbell or crowdion	A	0°
>1.2	⟨1 0 0⟩ dumbbell	A, B	54.74°

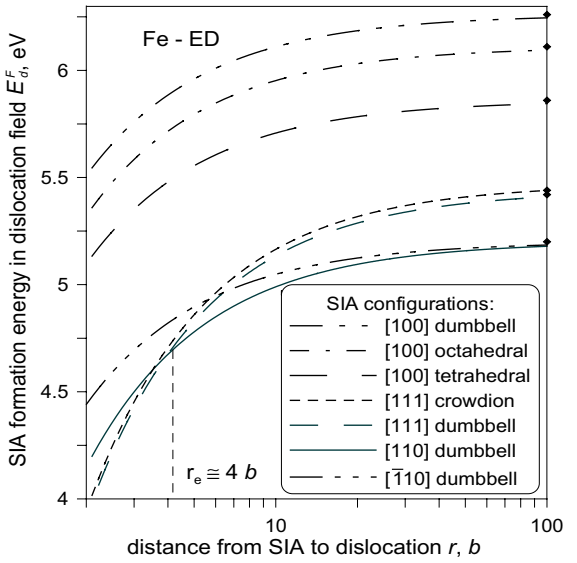

Fig. 2. Dependence of the formation energy E_d^F of various point defect configurations (SIA) on distance to the ED in $(\bar{1}\,1\,0)[1\,1\,1]$ slip plane in Fe. Diamonds are the values of the formation energy at infinity.

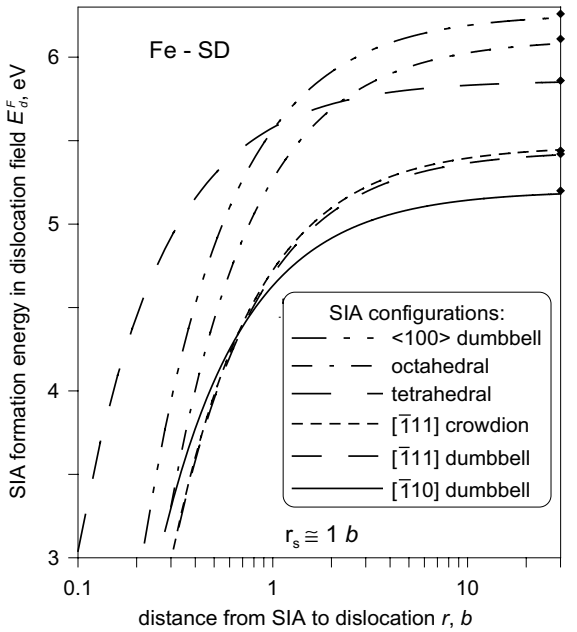

Fig. 3. Dependence of the formation energy E_d^F of various point defect configurations (SIA) on distance to the SD in $(\bar{1}\,1\,0)[1\,1\,1]$ slip plane in Fe. Diamonds are the values of the formation energy at infinity.

4.3. Critical densities of dislocations

Fields of dislocations govern the thermal mobility of point defects at some temperature T throughout the whole crystal volume at some critical density ρ_c of dislocations if the interaction energy E_{int} is larger than value of $k_B T$ in the whole crystal volume (k_B is Boltzmann's constant). So critical density ρ_c can be calculated as $\rho_c = \frac{1}{2S}$ where S is area of the capture range within which the interaction energy 'dislocation–point defect' is larger than value of $k_B T$.

Using the values of critical densities of dislocations, average distances from dislocations where dislocations control the thermal mobility of point defects at 20 °C (the interaction energy is larger than 0.025 eV) were calculated (Table 8). Obtained results show that if we take into account vacancy saddle point configurations, the ranges of the essential influence of dislocation fields on a vacancy increase in several times and the difference (bias factor) of this range between a SIA and a vacancy reduces. This difference is considerably less in V than in Fe as indicated in Table 8.

Analogous calculations on computer simulation of the interaction between an ED in the slip system ⟨1 1 1⟩{1 1 0} with SIAs and a vacancy in Fe crystal were performed in [20]. The results are qualitatively alike. Quantitative differences can be explained by essential differences in the relaxation volumes of SIAs and a

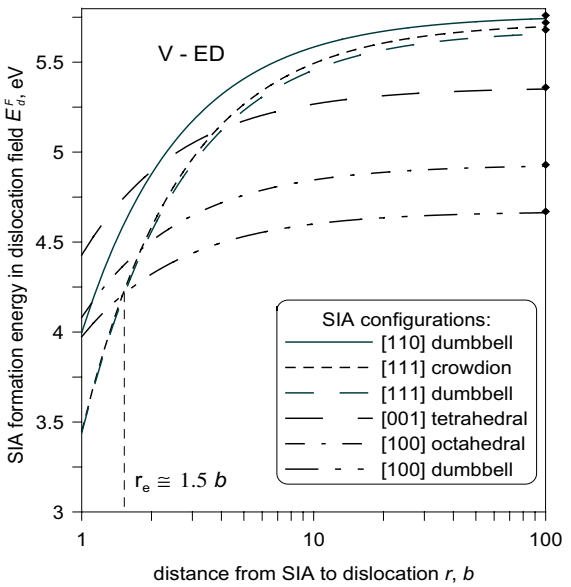

Fig. 4. Dependence of the formation energy E^F_d of various point defect configurations (SIA) on distance to the ED in $(\bar{1}\,1\,0)[1\,1\,1]$ slip plane in V. Diamonds are the values of the formation energy at infinity.

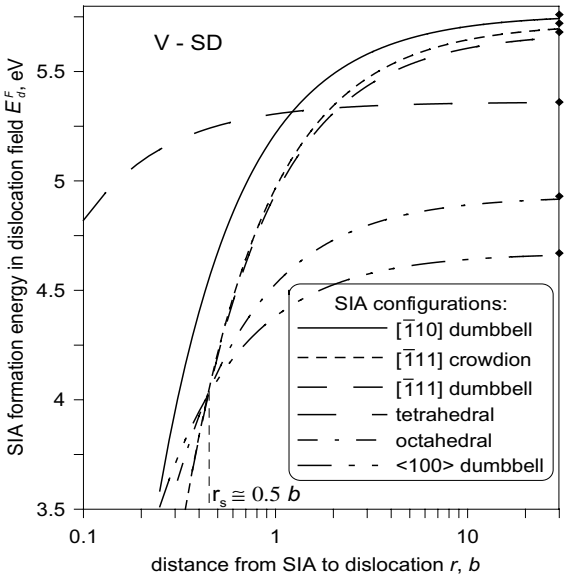

Fig. 5. Dependence of the formation energy E^F_d of various point defect configurations (SIA) on distance to the SD in $(\bar{1}\,1\,0)[1\,1\,1]$ slip plane in V. Diamonds are the values of the formation energy at infinity.

vacancy caused by use of another interatomic potential in [20].

5. Conclusion

(1) Elastic stress fields and energy factors of screw, mixed 45° and edge dislocations (SD, MD, ED) in basic slip systems $\langle 1\,1\,1\rangle\{1\,1\,0\}$ and $\langle 1\,1\,1\rangle\{1\,1\,2\}$ were calculated in the framework of anisotropic theory of elasticity for bcc V and Fe crystals. The straight form stability of dislocations was researched and was shown that dislocations in V and Fe crystals kept straight forms at temperature up to 1000 K.

(2) Crystallographic characteristics of self point defects (vacancies and SIAs as elastic dipoles of different symmetries in stable and metastable positions) were defined in bcc V and Fe crystals by computer simulation methods with use of suggested interatomic potentials (formation and migration energies, relaxation volumes, dipole tensors and their orientations). $\langle 1\,1\,0\rangle$ and $\langle 1\,0\,0\rangle$ dumbbells are the most stable point defect configurations in Fe and V crystals without internal stresses (without dislocations) respectively.

(3) Energies of elastic interaction between point defects and SDs, MDs and EDs in $\langle 1\,1\,1\rangle\{1\,1\,0\}$ slip system were calculated for bcc V and Fe crystals and essential influence of these interactions on the characteristics of point defects (formation energies, stable and unstable crystallographic configurations, diffusion ways) was shown.

The interaction of a dislocation with a SIA can lead to the stabilization of the SIA configurations that are metastable in the absence of dislocation elastic field.

Table 8
Average distance where dislocation in $(\bar{1}\,1\,0)[1\,1\,1]$ slip plane controls the thermal mobility of point defect at 20 °C ($E_{int} > 0.025$ eV), b

	Metal			
	Fe		V	
	SD	ED	SD	ED
Dumbbell[a]	20.2	74.5	10.2	24.0
Vacancy	1.0	5.6	0.5	9.6
Vacancy saddle point	4.4	12.6	6.9	19.8

Configuration: SD, ED.
[a] $\langle 1\,1\,0\rangle$ and $\langle 1\,0\,0\rangle$ dumbbell configurations for Fe and V, respectively (configurations with the lowest formation energy E^F).

In Fe crystal the region of stabilization of the crowdion and the ⟨1 1 1⟩ dumbbell configurations in the presence of a SD is $r_s \approx 1$ b, and the axis of the ⟨1 1 1⟩ dumbbell or the crowdion is oriented to the dislocation line. The region of stabilization of the crowdion and the ⟨1 1 1⟩ dumbbell configurations in the presence of an ED dislocation is $r_e \approx 4$ b, and the axis of the ⟨1 1 1⟩ dumbbell or the crowdion is oriented in the direction of the Burgers vector $\mathbf{b} = a/2$ [1 1 1].

Stable SIA configurations and orientations in the nearest-neighbourhood of SDs and EDs are the same in V and Fe crystals. In V crystal the radius-vectors delineating regions of stabilization take on values $r_s \approx 0.5$ b and $r_e \approx 1.5$ b for a SD and ED, respectively.

The migration of a SIA and a vacancy in V crystal does not qualitative differ from the migration in Fe crystal with the exception of the most stable SIA configuration far from dislocation (⟨1 0 0⟩ and ⟨1 1 0⟩ dumbbell configurations in V and Fe crystals, respectively).

The elastic field of an ED stabilizes the crowdion and ⟨1 1 1⟩ dumbbell configurations in the orientation such as to cause the SIA to 'hover' at some distance from the ED. The SD stabilizes these configurations in an orientation that makes it easier for the SIA to reach the dislocation.

The elastic field of the SD makes preferable the migration way of a vacancy to the dislocation. A vacancy 'hovers' at some distance from the ED.

(4) Critical densities of SD, MD and ED were defined at which their stress fields control thermal mobility of point defects throughout the whole crystal volume (the interaction energies of 'dislocation–point defect' are more than the energy of thermal fluctuations). Using these values, average distances from dislocations where they control thermal mobility of point defects at 20 °C were calculated.

(5) The interaction energies between vacancy saddle point configurations and dislocations in bcc crystals (V, Fe) are higher than the interaction energy between dislocations and vacancies in their stable configurations. Dislocations govern vacancy thermal mobility via vacancy saddle points. Taking into account the vacancy saddle point configurations, the range of the essential influence of dislocation fields on vacancies increases in several times and the difference of this range between a SIA and a vacancy (bias factor) reduces. This difference is considerably less in V than in Fe crystal.

References

[1] J.P. Hirth, J. Lothe, Theory of Dislocations, McGraw-Hill, New York, 1968.
[2] G. Leibfried, N. Brouer, Point Defects in Metals, Springer-Verlag, Berlin, 1978.
[3] V.L. Indenbom, V.M. Chernov, in: V.L. Indenbom, J. Lothe (Eds.), Elastic Strain Fields and Dislocation Mobility, North-Holland, Amsterdam, 1992, p. 517.
[4] L.I. Ivanov, Y.M. Platov, Radiation Physics of Metals and Applications, Interkontakt Nauka, Moscow, 2002 (in Russian).
[5] E. Kroener, Arch. Ration. Mech. Anal. 4 (1960) 18.
[6] V.L. Indenbom, V.I. Al'shits, V.M. Chernov, in: Computer Modeling of Defects in Crystals, Nauka, Leningrad, 1980, p. 23 (in Russian).
[7] V.M. Chernov, M.M. Savin, Phys. Stat. Sol. (a) 55 (1979) 13.
[8] V.M. Chernov, V.V. Ivanov, Cryst. Res. Technol. 19 (1984) 747.
[9] V.V. Ivanov, V.M. Chernov, Atom. Energ. 61 (1986) 422.
[10] D.J. Bolef, R.E. Smith, J.G. Miller, Phys. Rev. B 12 (1971) 4100.
[11] H.B. Huntington, in: F. Seitz, D. Turnbull (Eds.), Solid State Physics, vol. 7, Academic, New York, 1958, p. 274.
[12] V.A. Romanov, V.M. Chernov, A.O. Krutskikh, J. Nucl. Mater. 271&272 (1999) 274.
[13] V.A. Romanov, V.M. Chernov, A.O. Krutskikh, in: 5th IEA and JUPITER Joint Workshop on Vanadium for Fusion Applications, 2000, Tokyo, Japan, p. 317.
[14] R.G. McQueen, S.P. Marsh, J. Appl. Phys. 31 (1960) 1253.
[15] V.N. Zharkov, V.A. Kalinin, Uravneniya sostoyaniya tverdykh tel pri vysokikh davleniyakh i temperaturakh, Nauka, Moscow, 1968 (in Russian).
[16] J.H. Rose, J.R. Smith, F. Guinea, J. Ferrante, Phys. Rev. B 29 (1984) 2963.
[17] J.P. Biersack, J.F. Ziegler, Nucl. Instrum. and Meth. 194 (1982) 93.
[18] H.B. Huntington, G.A. Shirn, E.S. Wajda, Phys. Rev. 99 (1955) 1085.
[19] H.R. Schober, K.W. Ingle, J. Phys. F: Met. Phys. 10 (1980) 575.
[20] E. Kuramoto, K. Ohsawa, T. Tsutsumi, J. Nucl. Mater. 283–287 (2000) 778.